Absorption saturation mechanism for YAG:Cr^{4+} crystals

A. G. Okhrimchuk and A. V. Shestakov
Elements of Laser Systems Corporation, 3 Vvedensky Street, Moscow 117342, Russia
(Received 1 June 1999; revised manuscript received 10 August 1999)

Dependencies of optical transmittance and luminescence of YAG:Cr^{4+} crystals upon intensity of excitation at 1064 nm are investigated, when absorption of tetrahedrally coordinated Cr^{4+} ions (Cr^{4+} centers) is saturated. The spectroscopic model of Cr^{4+} center in YAG crystals is proposed. Absorption saturation of YAG:Cr^{4+} crystals at 1064 nm have to be described by two absorption cross sections $\sigma_{0\pi}=(3.9-5.0)\times10^{-18}\,\mathrm{cm}^2$ and $\sigma_{0\sigma}=(1.5-1.9)\times10^{-19}\,\mathrm{cm}^2$, arising from the D_{2d} local symmetry of Cr^{4+} centers. The cross sections slightly vary within the pointed range in dependency of level of the Cr dopant and a type of the Me^{2+} dopant (Mg^{2+} or Ca^{2+}). The absorption band centered at 1000 nm is basically due to $^3B_1(^3A_2)\rightarrow{}^3A_2(^3T_1)$ transition. Energy positions of $^3A_2(^3T_1)$ and $^3E(^3T_2)$ states are very close to each other, and the absorption band due to $^3B_1(^3A_2)\rightarrow{}^3E(^3T_2)$ transition is masked by the absorption due to $^3B_1(^3A_2)\rightarrow{}^3A_2(^3T_1)$ transition. The proposed model allows us to explain the dependence of the extent of luminescence polarization on the intensity of light exciting the YAG:Cr^{4+} crystal. Absorption from the metastable excited state $^3B_2(^3T_2)$ is negligible; its absorption cross section is less than $2\times10^{-20}\,\mathrm{cm}^2$. Linear losses from other centers are found in the crystals with a high level of the chromium dopant and with the calcium dopant.

I. INTRODUCTION

YAG:Cr^{4+} is an important crystal material for solid-state lasers. It is used for *Q* switching of Nd lasers at the 1000-nm region and for tunable laser operation in the 1350–1600-nm region.[1–5] Since this material was obtained and appropriately described[1], plenty of successful investigations have been made in the field of its spectroscopy,[6–16] but some principal questions remain obscured yet. Those are the energy levels scheme and the nature of residual absorption in regime, when the basic absorption is saturated.

Primarily the energy-level scheme was presented for the cubic symmetry approximation.[9–17] Later it was shown that the tetragonal distortion is of principal importance for correct description of optical transitions in YAG:Cr^{4+} crystal, because of strong polarization dependencies of the emission and absorption saturation.[4,6,14] In Refs. 4, 6, 14 a more detailed energy level scheme was proposed in the assumption of D_{2d} point-group symmetry, which corresponded better to the real symmetry of Cr^{4+} ions environment in the YAG crystal. This energy-level scheme was obtained for the approximation of strong crystal field in the crystal-field theory. In this approximation the 800–1200-nm absorption band, which is important for laser applications, belongs to $^3B_1(^3A_2)\rightarrow{}^3E(^3T_2)$ transition, and the 570–700-nm absorption band belongs to $^3B_1(^3A_2)\rightarrow{}^3A_2,{}^3E(^3T_1)$ transitions.

In the latest study[18] additional spectroscopic data have been obtained, in which the authors have pointed out that the energy level scheme has to be corrected within the same symmetry assumption, proposed earlier in Refs. 4, 6, and 14. The authors of Ref. 18 have supposed that the strong 800–1200-nm absorption band had to be attributed to $^3B_1(^3A_2)\rightarrow{}^3A_2(^3T_1)$ transition (see Fig. 1). This conclusion disagrees with the early assignment of the energy position of the $^3A_2(^3T_1)$ state. The authors suggested that the $^3T_1(^3F)$ state is much higher split than that assumed previously, and the energy position of $^3A_2(^3T_1)$ state is so low that it is very close to the position of the $^3E(^3T_2)$ state. Furthermore, as even in cubic symmetry approximation the $^3A_2\rightarrow{}^3T_1$ electric dipole transition is allowed, and the $^3B_1(^3A_2)\rightarrow{}^3E(^3T_2)$ electric dipole transition is only allowed for lower symmetry (D_{2d} in our case), they consider that the absorption from the $^3B_1(^3A_2)\rightarrow{}^3A_2(^3T_1)$ transition is considerably stronger than that from the $^3B_1(^3A_2)\rightarrow{}^3E(^3T_2)$ transition. So the latter absorption band is masked by the much stronger absorption band due to the $^3B_1(^3A_2)\rightarrow{}^3A_2(^3T_1)$ transition. This conclusion is mainly derived from the polarization dependencies observed in piezospectroscopic experiments. Nevertheless, we consider that the discourse adduced in Ref. 18 is based on the nonevidence assumption that the signs of elastic compliance coefficients

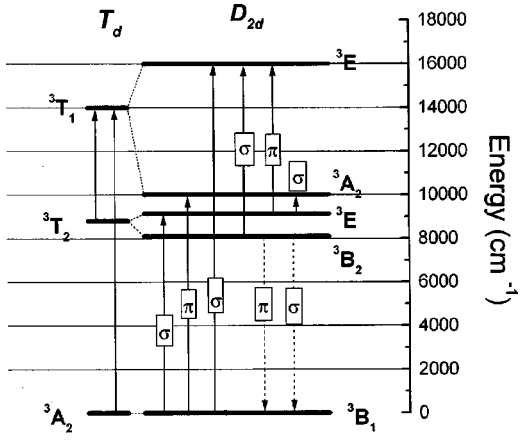

FIG. 1. Energy-levels scheme of the tetrahedrally coordinated Cr^{4+} ion in YAG crystal (D_{2d} point group of symmetry), and its correlation with a rough model of a cubic symmetry approximation (T_d point group). Allowed electronic transitions with absorption are shown by solid lines: (π) the electrical vector of light is parallel to the S_4 local symmetry axis, (σ) it is perpendicular to the S_4 axis. Emission transitions are forbidden between pure electronic states and come from vibration assistance.

for a tetrahedron occupied by a Cr^{4+} ion are the same as for the whole YAG crystal. Furthermore, the sharp lines centered at 1077 and 1114 nm were investigated only, so even if we assume that these lines belong to the $^3B_1(^3A_2) \rightarrow {}^3A_2(^3T_1)$ transition, the rest of the wide intensive band absorption around 1000 nm may belong to the $^3B_1(^3A_2) \rightarrow {}^3E(^3T_2)$ transition. Therefore additional spectroscopic data on this absorption band are needed.

The authors of Ref. 18 also reference their earlier work,[19] devoted to investigation of absorption saturation under polarized light at 1064 nm. But no serious attempts were made in this work to assign the saturable absorption band to one or another transition. Thus we consider that it is important to test YAG:Cr^{4+} crystals in such experiments carefully, because absorption saturation plays a principal role for this laser material.

Heretofore we have observed a dependence of polarization extent of luminescence upon intensity of 1064-nm pumping.[20] To explain this dependence we suppose that two different electronic-vibronic transitions are responsible for absorption saturation in the Cr^{4+} center. This fact does not contradict to the energy-level scheme presented in Ref. 18, and it indicates that the simple model with one absorption transition in the Cr^{4+} center cannot describe absorption saturation in YAG:Cr^{4+} crystal adequately.

To study the question about the energy-level scheme and the absorption saturation mechanism in YAG:Cr^{4+} crystal, we have undertaken careful investigations of YAG:Cr^{4+} absorption saturation under plane-polarized pumping light at 1064 nm for cw and for pulsed regimes. Under these conditions we have studied both polarized luminescence in the 1350–1700-nm region and transmittance for linear polarized light at 1064 nm.

II. THEORETICAL APPROACH

Consider propagation of plane-polarized light in a crystal with absorption by identical optical centers, but with different orientations relative to crystallographic axes, and this circumstance is a reason for differences in absorption probabilities of the centers. We assume that wavelength width of the light is rather less than the wavelength width of the absorption band, and the centers have the quasi-four-level energy scheme, additionally including absorption from a metastable excited state (ESA). Such situation is common for impurity ions of transition *d* elements. Absorption saturation is due to accumulation of the centers at the metastable level, and consequently to depletion of ground state.

We assume that relaxation after ESA goes back to the metastable excited state with relaxation time is rather short in comparison with the lifetime τ_1 of the metastable excited state. ESA is not saturated, so the density in the higher excited state is negligible in comparison with densities in the ground state and in the metastable excited state. Thus the following rate equation describes light propagation and evolution of the ground-state densities N_{0i}.

$$\frac{1}{C}\frac{\partial I}{\partial t}+\frac{\partial I}{\partial z}=-\sum_{i=1}^{m}(\sigma_{0i}N_{0i}+\sigma_{1i}N_{1i})I-\alpha_r I, \tag{1}$$

$$\frac{\partial N_{0i}}{\partial t}=-\sigma_{0i}N_{0i}\frac{I}{h\nu}+\frac{N_{1i}}{\tau_1}, \tag{2}$$

$$N_{0i}+N_{1i}=N_i, \quad i=1,2\ldots m, \tag{3}$$

where $I(z,t)$ is the intensity of the light; m is the number of types of center orientations; $N_i(z,t)$ is the total concentration of centers with *i*-type orientation, $N_{0i}(z,t)$ and $N_{1i}(z,t)$ are concentrations of the centers in ground and metastable excited states, correspondingly, σ_{0i} and σ_{1i} are absorption cross sections of *i*-type oriented centers for transitions from ground state and metastable excited state, correspondingly (σ_{0i} and σ_{1i} generally depend also upon the direction of electrical vector of the light), α_r is coefficient of linear losses, and $h\nu$ is the energy of a light quantum.

Further we consider the two degenerate cases corresponding to real experiments, which we have accomplished with YAG:Cr^{4+} crystals. One case corresponds to a short pulse of the exciting light and other case corresponds to the cw exciting light.

When interaction time of the light pulse with the crystal Δt is rather less than the metastable lifetime τ_1, it is convenient to put in a fluence of the pulse $U(z)$:

$$U(z)=\int_{-\Delta t}^{0} I(z,t)dt. \tag{4}$$

Here we assume that the interaction is over at $t=0$. In this case (2) can be easily integrated, if one assume that spontaneous relaxation of metastable state is slow in comparison with the excitation time ($\tau \gg \Delta t$):

$$N_{0i}(z,0)=N_i\exp[-U(z)\sigma_{0i}/h\nu], \tag{5}$$

$$N_{1i}(z,t)=[N_i-N_{i0}(z,0)]\exp(-t/\tau_1), \quad t>0. \tag{6}$$

A meaning of N_{0i} is the lowest population density of the ground state during the entire cycle of the excitation and relaxation.

We obtain from Eqs. (2)–(5)

$$dU=\sum_{i=1}^{m} N_i\left\{h\nu\left(1-\frac{\sigma_{1i}}{\sigma_{0i}}\right)\left[\exp\left(-\frac{U\sigma_{0i}}{h\nu}\right)-1\right]-\sigma_{1i}U\right\}dz - \alpha_r U dz. \tag{7}$$

Now we can calculate transmittance of low intensity probe beam $T(U_{on},t)$, which does not disturb the population densities of the ground and excited states:

$$T(U_{on})=T_0\cdot\exp\{-\xi\cdot\exp(-t/\tau_1)\}, \tag{8}$$

where T_0 is the transmittance of an unexcited crystal:

$$T_0=\exp\left(-\sum_{i}^{m}\sigma_{0i}N_i-\alpha_r d\right), \tag{9}$$

$\xi(U_{on})$ is the parameter characterizing an extent of absorption saturation of the crystal:

$$\xi(U_{on})=\int_0^d\sum_{i=1}^{m}[(\sigma_{0i}^*-\sigma_{1i}^*)(N_i-N_{0i})]dz, \tag{10}$$

TABLE I. Specifications of the samples and results of the investigations. The errors are calculated when standard errors for each experimental point were assumed to be the same and equal to the root mean square of deviations between theoretical and experimental points.

Initial samples data						Results of the experiment with transmittance						Results of the experiment with luminescence	
Crystal No.	[Cr] 10^{19} cm^{-3}	[Mg] 10^{19} cm^{-3}	[Ca] 10^{19} cm^{-3}	T_{ht} grad K	T_0 %	$\sigma_{0\pi}$ 10^{-18} cm^2	$\sigma_{1\pi}$ 10^{-20} cm^2	$\sigma_{0\sigma}$ 10^{-20} cm^2	$\sigma_{1\sigma}$ 10^{-20} cm^2	k	τ μs	A_σ/A_π	$\sigma_{0\sigma}$ 10^{-20} cm^2
B85-1	0.9	1.4		1550	63.5	3.93 ± 0.17	<2	16.1 ± 0.3	<1	>150	4.2 ± 0.1		
B85-5	0.9	1.4		1800	64.4	4.44 ± 0.11	<1.5	15.1 ± 0.3	<2.3	>200	4.3 ± 0.1	0.15 ± 0.01	18 ± 3
K1	19	2.4		1550	43.7	4.52 ± 0.22		15.2 ± 0.4		55 ± 20	3.93 ± 0.02		
B2-13	0.4		3.5	1550	38.5	5.04 ± 0.14		19.0 ± 0.2		11 ± 0.7	4.18 ± 0.02		

where σ_{0i}^* and σ_{1i}^* are absorption cross sections of active centers for interaction with the probe beam. If polarization of the probe light coincides with polarization of the pump light, $\sigma_{0i}^*=\sigma_{0i}$ and $\sigma_{1i}^*=\sigma_{1i}$.

Consider pumping by continuous-wave light and the polarization extent of luminescence. We assume that the integral luminescence from the whole excited region of the sample is detected, thus we must account for the spatial distribution of the pump beam intensity $I(z,r,\varphi)$. Let us assume a Gaussian pump beam:

$$I(z,r)=\frac{2P(z)}{\pi\omega^2(z)}\exp\left(-\frac{2r^2}{\omega^2(z)}\right), \tag{11}$$

where P is the power of the beam, ω is the waist radius.

So as in the steady-state regime $\partial N_{0i}/\partial t=0$, we obtain from Eqs. (2) and (3)

$$N_{1i}(z,r)=\frac{I(z,r)N_i(z,r)\sigma_{0i}\tau_1/h\nu}{1+I(z,r)\sigma_{0i}\tau_1/h\nu}. \tag{12}$$

Substituting Eqs. (3), (11), and (12) into Eq. (1) and taking integral over the cross section of the beam we will obtain the equation for power $P(z)$:

$$dP=-\sum_{i=1}^{m}N_i\left[\frac{\pi\omega^2(z)h\nu}{2\tau_1}\left(1-\frac{\sigma_{1i}}{\sigma_{0i}}\right)\ln\left(1+\frac{2\tau_1\sigma_{0i}P(z)}{\pi\omega^2(z)h\nu}\right)+P(z)\sigma_{1i}\right]dz-\alpha_r P(z)dz. \tag{13}$$

Integrating both parts of Eq. (12) over the cross section of the beam we obtain the linear density of i-type excited centers:

$$M_{1i}(z)=\int_0^\infty\int_0^{2\pi}N_{1i}(z,r)r\,dr\,d\varphi=\frac{\pi\omega^2(z)N_i}{2}\ln\left(1+\frac{2\tau_1\sigma_{0i}P(z)}{\pi\omega^2(z)h\nu}\right). \tag{14}$$

Now we can calculate the dependence of the extent of luminescence polarization p upon power of the beam falling on the sample $P_{on}=P(0)$:

$$p(P_{on})=\frac{L_{paral}}{L_{perp}}=\frac{\sum_{i=1}^{m}A_{i,paral}\int_0^d M_{1i}(z)dz}{\sum_{i=1}^{m}A_{i,perp}\int_0^d M_{1i}(z)dz}, \tag{15}$$

where L_{paral} and L_{perp} are intensities of luminescence components polarized parallel and perpendicular to polarization of the pumping light correspondingly; $A_{i,paral}$ and $A_{i,perp}$ are probabilities of spontaneous emission for i-type center with polarization parallel and perpendicular to polarization of the pumping light, correspondingly.

III. THE SAMPLES INVESTIGATED

Specifications of investigated crystals are summarized in Table I. We have tried to investigate all important kinds of YAG:Cr^{4+} differed by types and levels of doping and temperature of heat treatment.

A magnesium or calcium dopant is usually used to cause chromium to change valence from 3 to 4. As we investigated the YAG:Cr, Mg, so as the YAG:Cr, Ca crystals. Nevertheless, as far as we know, differences in spectroscopic properties of these crystals were not reported up to now. We have tried to find such differences.

It was found that there are some additional centers in the crystals with high chromium dopant level.[13] It has been supposed that these additional centers could be complex centers consisting of two ions such as Cr^{4+}, Cr^{3+}, or Me^{2+}. Thus it is also interesting to investigate crystals with low as well as with high chromium dopant level (compare samples N85 and N1).

Samples were prepared as it was described in Ref. 21. The crystals were grown by Chochralsky technique along [100] crystallographic axis. YAG:Cr^{4+} plates with nearly 3-mm thickness were cut from a bowl so that the [100] crystallographic axis was perpendicular to a base plane of the plate. The plates were heat treated in air. As temperature of the heat treatment could affect the process of the complex center generation we have investigated samples cut out from one bowl, but heat treated at different temperature T_{ht} (samples N85-1, N85-5).

IV. SCHEMES OF THE EXPERIMENTS AND MEASUREMENTS PROCEDURES

Pump-probe technique is applied to investigate dependence of transmittance of the crystals upon energy fluence. The experimental setup is shown in Fig. 2. Pump and probe

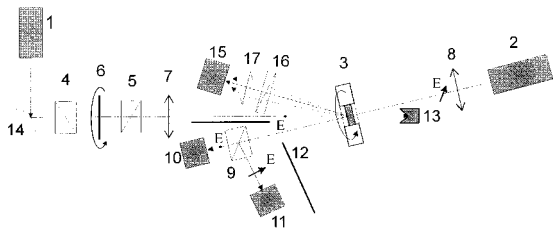

FIG. 2. Experimental setup for investigation of transmittance. The sample is excited by pulses of 1.064-μm linear polarized light of *Q*-switched Nd:YAG laser 1. Pulse duration is equal to 30 ns, repetition rate is equal to 10 Hz. Fluence of the pump light is controlled by polarization attenuator, consisting of the rotating quartz birefringent $\lambda/2$ plate 6 and Glan prisms 4 and 5. Lens 7 focused the pump beam on the sample with 1.5-mm sport size. Polarization of the pump light is perpendicular to the plane of the setup. The samples are mounted in holder 3. Transmittance of the sample is measured with a 1.064-μm cw diode pumped Nd:YAG laser 2. Lens 8 focused the single transverse mode probe beam of this laser in the spot with nearly 0.1-mm diameter. Axis of the probe beam is perpendicular to the polished planes of the sample, and so it is parallel to the [100] crystallographic axis.

beams intersect in the volume of a sample. The fluence distribution of the pumping beam in cross section at the sample location is tested by a video camera. It has a quasiflat top with cross deviations less than 5% within the confines of probe beam cross sweeping caused by divergence between the pump and the probe beams.

Orientation of the sample has been adjusted so that crystallographic axis [010] or [001] is parallel to the vertically oriented electrical vector of the pump light. This alignment has been done due to polarization properties of YAG:Cr^{4+} luminescence reported in Refs. 4, 6, 13, and 14. Ge photodiode 15 with interference filter 18 and film polarizer 16 is placed in front of the sample to detect luminescence of the last. The polarizer 16 transmits horizontally polarized radiation of luminescence, that is, polarized perpendicular to polarization of pump light. Minimum of luminescence intensity is achieved by tuning the holder 3 with the sample around the probe beam optical axis. Such orientation corresponds to maximum of polarization extent of luminescence and consequently to the required orientation of the sample. Indeed, Cr^{4+} centers differ by orientations in the three equal groups,[13] and we would obtain the maximum polarization extent of the luminescence, if mainly one of the groups will be excited. So as the centers are oriented along the main crystallographic axes of YAG, the maximum polarization extent of luminescence is reached when the electrical vector of pump light is parallel to one of the main crystallographic axes, that is [010] or [001], if a sample is tuned around the [100] axis.

The plane of polarization of the probe beam is inclined nearly by 45 grad relative to vertical. The Glan prism 9 is used to separate vertical and horizontal polarizations of the probe beam passed through the sample. Thus the sample is tested by both polarization components of the probe beam; one has parallel polarization relative to polarization of pump beam and another has perpendicular polarization. The separated polarization components of the probe beam are detected by different Ge photodiodes 10 and 11.

The absolute small signal transmittance of the samples T_0 is measured by a spectrophotometer. It is necessary to obtain the transmittance kinetics curves $T(U_{\rm on},t)$ by normalizing of the kinetic curves of the probe beam intensity. The resulting typical kinetics are shown in Fig. 3.

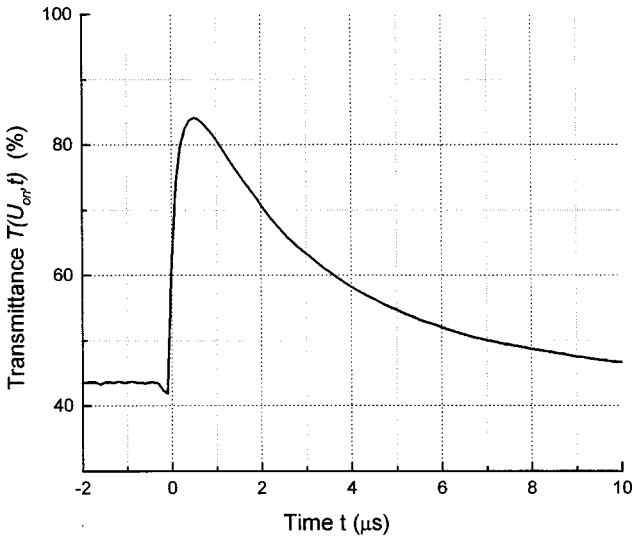

FIG. 3. The typical kinetics curve of transmittance.

We fit an experimental kinetics of transmittance $T(U_{\rm on},t)$ by the theoretical expression (8) at the interval of time from 1.5 to 100 μs, where time resolution does not distort the kinetics curve.

As a result of this fitting procedure we have obtained the parameters ξ, τ_1 and have restored the transmittance $T(U_{\rm on},0)$ for the moment, when the excited-state population N_{1i} is maximal. Further we will refer to the obtained dependences $T(U_{\rm on},0)$ as experimental ones (Fig. 4). It was found that the decay time τ_1 did not depend on the fluence $U_{\rm on}$. The values of decay time τ_1 are presented in Table I. The decay time τ_1 is significantly lower for the sample $K1$ with high chromium dopant than for other samples, and its value well agrees with the results obtained for luminescence decay.[13]

The experiment setup for investigation of polarization properties of the luminescence is shown in Fig. 5. The dependence of the extent of luminescence polarization upon the power of 1.064-μm light falling on the sample is investigated in the regime of absorption saturation. The luminescence component with the same polarization as pumping light $L_{\rm paral}$ and one with perpendicular polarization $L_{\rm perp}$ are separately detected. The extent of luminescence polarization is calculated by the formula

$$p = L_{\rm paral}/L_{\rm perp}. \tag{16}$$

The power of pumping light is controlled by the quartz acoustic-optic deflector 2. The laser beam is deflected in the first-order pass through hole 3. Signals from photodiodes are simultaneously recorded in different channels of a digital oscilloscope. To avoid heating of the sample, measurements are conducted for pulsed pumping with the pulse duration of about 25 ms and repetition rate of about 20 Hz. Position of the sample is adjusted by its replacement along the optical axis of the pumping beam to reach maximum effect of the absorption saturation, which is controlled by a minimum of

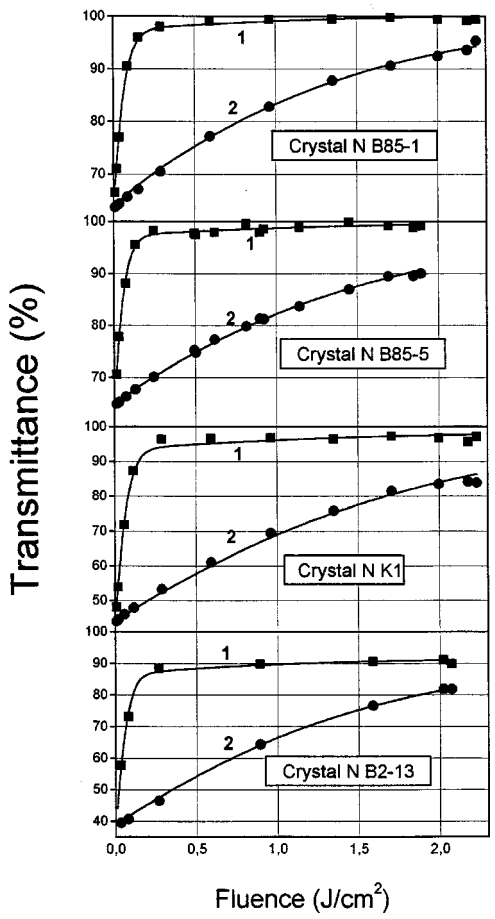

FIG. 4. The dependences of transmittance on the fluence for the probe beam polarized parallel (1) and perpendicular (2) to the pump light polarization. Points: experiment. The solid line is the theory curve fitted to the experimental data. The dashed line is the same theory curve, but without account of pumping light contribution ($B=0$).

the luminescence intensity. The sample was rotated in holder 6 around the optical axis as in experiments with transmittance to adjust orientation of its crystallographic axes relative to the electrical vector of the pumping light, so that a [100]-type axis is parallel to the pumping light electrical vector. The results of the experiment are presented in Fig. 6.

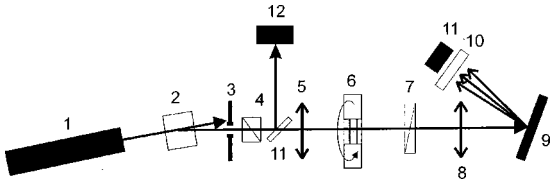

FIG. 5. The experiment setup for investigation of polarization properties of luminescence. Plane polarized beam from cw TEM_{00} Nd:YAG laser 1 was focused by 10-cm lens 5 in the volume of the sample placed in the holder 6. Waist diameter of the laser beam was 30 μm. Polished faces of the crystal were perpendicular to the beam axis. Wide band luminescence of the sample was detected by Ge photodiode 11. Film polarizer 7 was used to separate polarization components of the luminescence. An interference filter 10 with cut-off wavelength 1.35 μm was used to block pump light.

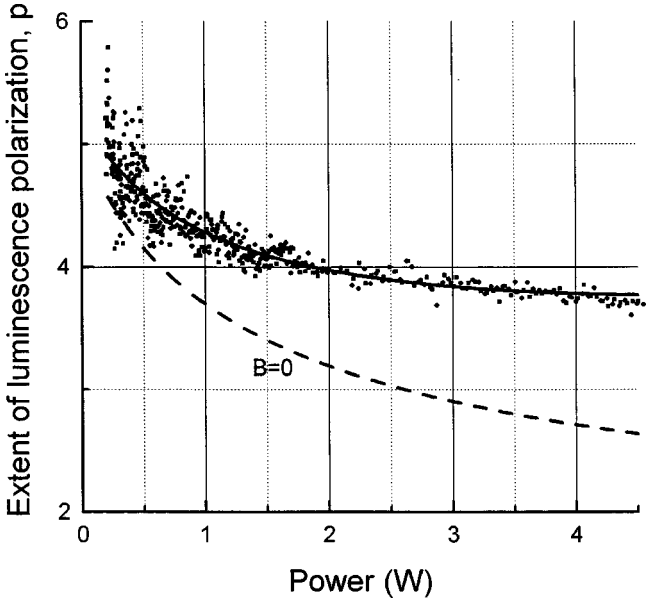

FIG. 6. Dependence of polarization extent of luminescence on the power of the beam falling on the crystal. Points: experiment. Solid line: the theory curve fitted to the experimental one.

V. INTERPRETATIONS OF EXPERIMENTAL RESULTS AND DISCUSSION

It has been established that the D_{2d} symmetry point group well describes the polarization properties of the Cr^{4+} center emission and absorption.[6,13,14,19] It is considered that all Cr^{4+} centers are identical and differ by orientations only. We believe that our experimental data affirm the earlier point of view on the type of local symmetry of the Cr^{4+} center, but the energy positions of the $^3A(^3T_1)$ state have to be corrected compared to those assumed in Refs. 6, 13, and 14.

In the case of D_{2d} symmetry, the electronic dipole transitions between any two electronic states must be subdivided by polarization into two types. The first type is for the electric-field vector of light being parallel the S_4 local axis of symmetry, and the second type is for an electrical vector being perpendicular to this axis. We denote the absorption cross section for the first type of transitions by $\sigma_{0\pi}$ and $\sigma_{1\pi}$ from the ground state and from the first excited state correspondingly, and for the second type transitions by $\sigma_{0\sigma}$ and $\sigma_{1\sigma}$. There are three types of center orientations in the crystal lattice of YAG, that is, along three main crystallographic axes, so the centers are subdivided in three equal subsets by orientation attribute (see Fig. 7). Thus to apply Eq. (1)–(15) we must assume $m=3$. In our experiments the electric vector of the pump light is parallel to a main crystallographic axis, hence it is parallel to the S_4 axes of a $\frac{1}{3}$ part of all centers ($i=1$) and perpendicular to the S_4 axes of the $\frac{2}{3}$ remainder of all centers ($i=2,3$). Application of Eq. (10) to the scheme of our experiment gives for the probe beam components polarized parallel and perpendicular to polarization of the pump light, correspondingly,

$$\xi_{\mathrm{par}}(U_{\mathrm{on}})=\int_0^d[(\sigma_{0\pi}-\sigma_{1\pi})(N-N_{0z})+2(\sigma_{0\sigma}-\sigma_{1\sigma})\times(N-N_{0xy})]dz, \tag{17}$$

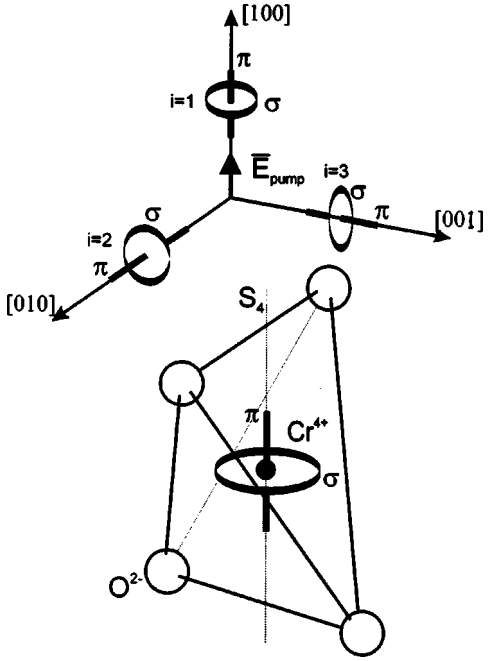

FIG. 7. The structure scheme of the Cr^{4+} center and three orientation types of the Cr^{4+} centers in the YAG crystal. π, σ are the local symmetry axis and the local symmetry plane of the Cr^{4+} center; π is parallel to the S_4 local symmetry axis, σ is perpendicular to the S_4 local symmetry axis.

$$\xi_{\mathrm{perp}}(U_{\mathrm{on}}) = \int_0^d [(\sigma_{0\sigma} - \sigma_{1\sigma})(N - N_{0z}) + (\sigma_{0\pi} - \sigma_{1\pi} + \sigma_{0\sigma} - \sigma_{1\sigma})(N - N_{0xy})]dz. \tag{18}$$

Numerical solution of Eqs. (5), (7)–(9), (17), and (18) results in theoretical dependencies of transmittance of the probe beam upon the pump fluence $T(U_{\mathrm{on}})$. These dependencies are used in fitting experimental data.

To characterize relative quantity of linear losses in the YAG:Cr^{4+} crystal we introduce the ultimate contrast k_u:

$$k_u = -\frac{\ln(T_0)}{\alpha_r}, \tag{19}$$

where α_r are linear losses belonging to other types of centers.

If the polarization of the probe beam is parallel to the polarization of the exciting light, the absorption in the samples B85-1 and B85-5 tends to zero for the energy fluence exceeding 1 J/cm^2, while the absorption of other samples goes to nonzero values in these conditions (Fig. 4). Therefore we assume that this residual unsaturable absorption is not due to transitions in the Cr^{4+} center, but belongs to other centers.

We fit the theoretical dependence to the experimental data for samples B85-1 and B85-5 by varying parameters $\sigma_{0\pi}$, $\sigma_{0\sigma}$, and α_r, while $\sigma_{1\pi}$ and $\sigma_{1\sigma}$ are set to zero. The results of least-square fittings are introduced in Table I. The mean value of unsaturable losses α_r is found to be zero accurate within an experimental error. The low limit for the ultimate contrast k_u is evaluated by formula (19), when the error for the linear losses α_r is taken as the upper limit of α_r. The upper limits for the cross sections $\sigma_{1\pi}$ and $\sigma_{1\sigma}$ are obtained in the fitting procedures when they are varied with fixed $\sigma_{0\pi}$, $\sigma_{0\sigma}$, and α_r, determined in the previous fitting.

Fitting to experimental data for transmittance of samples K1 and B2-13 is also made with the assumption that $\sigma_{1\pi}$ and $\sigma_{1\sigma}$ equals to zero. As one can see from Table I, the fit gives slightly different values for the cross sections $\sigma_{0\pi}$ and $\sigma_{0\sigma}$ for different samples. We suggest that these differences arise from variations of crystal-field strength, which are due to dopants of Cr and Me^{2+}.

Thus we obtain that the absorption cross section of a center for electrical vector parallel to the S_4 axis $\sigma_{0\pi}$ is about 30 times higher than absorption cross section for perpendicular directions $\sigma_{0\sigma}$. This result is the same as predicted by the group theory for the $^3B_1(^3A_2) \rightarrow {}^3A_2(^3T_1)$ transition.[13,14] So we obtain a clear demonstration that absorption at 1064-nm wavelength mainly belongs to transition from the ground state to the $^3A_2(^3T_1)$ excited state and corroborate the conclusion obtained in Ref. 18. The found value of the absorption cross section for polarization perpendicular to the local axis S_4 $\sigma_{0\sigma}$ is consistent with transition $^3B_1(^3A_2) \rightarrow {}^3E(^3T_2)$, allowed by tetragonal distortion along S_4 axis, and the $^3B_1(^3A_2) \rightarrow {}^3A_2(^3T_1)$ transition could also contribute to the absorption for this polarization. The obtained cross section of base saturable transition $\sigma_{0\pi}$ agrees quite well with those obtained in Ref. 21 (5×10^{-18} cm^2), Ref. 19 (5.7×10^{-18} cm^2), and Ref. 3 (3.0×10^{-18} cm^2) for a simple model, when only one transition assumed participates in absorption saturation.

Similar experiments were done in Ref. 22, but we consider that in those experiments the excitation density was not high enough to make clear assignment of the 800–1200-nm absorption band and the authors did not make any speculations about this.

The dependence of luminescence polarization on the power of pumping light observed in our experiment (Fig. 6) confirms the consideration that the absorption is due to two transitions with different cross sections and polarization. Such dependence could not exist, if the absorption is due to only one type transition. Indeed, if the absorption would be due to $^3B_1(^3A_2) \rightarrow {}^3A_2(^3T_1)$ transition, the centers of only one type [with the S_4 axes parallel to electrical vector of pumping light ($i=1$, Fig. 7)] would be excited, and the extent of luminescence polarization would depend only on intrinsic properties of the center. When we assume the absorption to be due to $^3B_1(^3A_2) \rightarrow {}^3E(^3T_2)$ transition, the centers of two types [with S_4 axes perpendicular to electrical vector of pumping light ($i=2,3$)] would be excited with the same probability, and the extent of luminescence polarization would depend again only on intrinsic properties of the center. The situation differs for the model, presented to describe absorption saturation in our work. In this case the centers of one type ($i=1$) are predominatingly excited when the pumping light intensity is low, and the centers of other types ($i=2,3$) will be excited additionally as pumping light intensity rises. Thus anisotropy in the excited center subset is highest for the low intensity pumping light, and it falls down when the intensity of the pumping light increases. As a result, decrease of the extent of the luminescence polarization must be observed.

Equations (13)–(15) are used to calculate theoretical dependence of the extent of the luminescence polarization upon the power of continuous-wave exciting light $p(P_{on})$. Equation (15) has to be adapted for the YAG:Cr^{4+} crystal. Analogic to the description of polarization properties of absorption of a separate center, the luminescence of each center can be characterized by two components of emission probabilities only; one is for electrical vector of emission parallel to the S_4 local symmetry axis A_π and other is for electrical vector of emission perpendicular to this axis A_σ. Thus we obtain

$$p(P_{on})=\frac{2(A_\pi/A_\sigma)\int_0^d M_{1xy}dz+\int_0^d M_z dz+BP_{on}}{(A_\pi/A_\sigma)\left[\int_0^d (M_{1xy}+M_{1z})dz\right]+\int_0^d M_{1xy}dz}. \tag{20}$$

Only the ratio A_π/A_σ could be obtained by analyzing the dependence of the extent of luminescence polarization p upon the power of pumping light. The additional term BP_{on} is introduced in Eq. (20) to allow the parasitic signal from pumping light to partially pass through filter 10 (Fig. 5).

Equations (13), (14), and (20) are applied to fit the theoretical dependence of the extent of luminescence polarization to the experimental one shown in Fig. 6. Varied parameters are the absorption cross section $\sigma_{0\sigma}$, the ratio of emission probabilities A_π/A_σ, and the B coefficient. The absorption cross section $\sigma_{0\pi}$ and relaxation time τ_1 are fixed and accepted to be equal to those obtained in the experiments with transmittance (see Table I). As follows from its results, excited-state absorption is negligible, so absorption cross sections for transitions from the excited state are assumed equal to zero. The initial transmittance T_0 is defined by a spectrophotometer. Fitting procedure results are summarized in Table I. The found value for the absorption cross section $\sigma_{0\sigma}$ agrees well with those independently obtained in the experiments with transmittance. The found ratio of emission probabilities $A_\sigma/A_\pi=0.15$ shows that the emission with electrical vector parallel to local axis S_4 is more probable. The ratio of absorption probabilities for different polarizations ($\sigma_{0\sigma}/\sigma_{0\pi}=0.034$) is rather less than A_σ/A_π (see Table I). It is not a surprise, because the $^3B_1(^3A_2)\rightarrow{}^3A_2(^3T_1)$ electronic transition working in absorption is allowed for the electrical vector parallel to the S_4 axis, and is forbidden for other directions. So only electron-vibronic interaction and mixing of electronic states can lower differences between probabilities for different polarizations. The pure electronic transition $^3B_2(^3T_2)\rightarrow{}^3B_1(^3A_2)$ working in emission is forbidden for any state of polarization, that is, there are no polarization preferences. We believe that it is partly allowed by electron-vibronic interaction.

The conclusion that the absorption at 1064 nm predominantly belongs to the $^3B_1(^3A_2)\rightarrow{}^3A_2(^3T_1)$ transition can be expanded on the whole wide absorption band near 1000 nm. In the 800–1150-nm region a shape of the polarized excitation spectrum of polarized luminescence did not depend on the relative polarizations of the exciting light and the detected luminescence, i.e., the extent of luminescence polarization did not depend on the excitation wavelength.[6] Thus the whole 800–1150-nm absorption band belongs to transitions with the same symmetry properties. Symmetry properties of the $^3B_1(^3A_2)\rightarrow{}^3A_2(^3T_1)$ and $^3B_1(^3A_2)\rightarrow{}^3E(^3T_2)$ transition are basically different (see Fig. 1), so the $^3B_1(^3A_2)\rightarrow{}^3E(^3T_2)$ transition contributes a negligible part in absorption band around 1000 nm.

Energy positions of electronic states of the Cr^{4+} ion in the crystal field with D_{2d} symmetry were calculated for the model of pure ion interaction,[6,13] that is, ligands O^{2-} were assumed as point charges. Results of these calculations had pointed out that the $^3A_2(^3T_1)$ state lay at 14 000 cm^{-1}. This does not agree with the results of the present study, which shows that wide absorption centered at the 1000 nm (10 000 cm^{-1}) band is due to the $^3B_1(^3A_2)-{}^3A_2(^3T_1)$ transition, and consequently the $^3A_2(^3T_1)$ state lies near 9000 cm^{-1}. Energy-level calculations of the Cr^{4+} ion are reported in Ref. 23 for the more precise model of charge exchange, when covalence of ligand and Cr^{4+} ion interaction is taken into account. In accordance with the results of this work, the $^3A_2(^3T_1)$ state lies at 9384.3 cm^{-1}. This is in good agreement with our present results. Thus covalence plays a principal role for the Cr^{4+} center.

The obtained differential Eqs. (7) and (13) describe light propagation in crystals with saturable absorption for pulsed and cw regimes correspondingly, when a low symmetry of active centers is accounted for. Application of Eq. (7) to a YAG:Cr^{4+} crystal plate with thickness l gives for plane polarized pulsed light, propagating along the [100] crystallographic axis and polarized along the [010] axis:

$$dU=\frac{\ln(T_0)}{l}\left[\frac{h\nu}{\sigma_\pi+2\sigma_\sigma}(e^{-U\sigma_\pi/h\nu}+2e^{-U\sigma_\sigma/h\nu}-3)-\frac{U}{k_u}\right]dz \tag{21}$$

and it polarized along the [011] crystallographic axis:

$$dU=\frac{\ln(T_0)}{l}\left[\frac{h\nu}{\sigma_\pi+2\sigma_\sigma}(2e^{-U\sigma_\pi/2h\nu}+e^{-U\sigma_\sigma/h\nu}-3)-\frac{U}{k_u}\right]dz. \tag{22}$$

All notations in Eqs. (21) and (22) correspond to Table I.

VI. CONCLUSIONS

The spectroscopic model of Cr^{4+} center in YAG crystal is proposed. It allows us to comprehensively describe absorption saturation in this crystal including polarization effects.

Absorption saturation of the YAG:Cr^{4+} crystal at the 1064-nm wavelength must be described by two absorption cross sections $\sigma_{0\pi}=(3.9–5.0)\times10^{-18}\,cm^2$ and $\sigma_{0\sigma}=(1.5–1.9)\times10^{-19}\,cm^2$, arising from D_{2d} local symmetry of the tetrahedrally coordinated Cr^{4+} ion. These cross sections correspond to different directions of light polarization relative to a local symmetry axis S_4 of the Cr^{4+} center. The absorption band centered at 1000 nm is basically due to the $^3B_1(^3A_2)\rightarrow{}^3A_2(^3T_1)$ transition. Energy positions of $^3A_2(^3T_1)$ and $^3E(^3T_2)$ states are very close to each other, and the absorption band due to the $^3B_1(^3A_2)\rightarrow{}^3E(^3T_2)$ transition is masked by absorption due to the $^3B_1(^3A_2)\rightarrow{}^3A_2(^3T_1)$ transition. Covalence must be taken into account when the energy-level scheme of the tetrahedrally coordinated Cr^{4+} ion in the YAG crystal is calculated. The pro-

posed model allows us to explain the dependence of the extent of the luminescence polarization on the light intensity exciting the YAG:Cr^{4+} crystal.

The absorption cross sections for $^3B_1(^3A_2) \rightarrow {}^3A_2(^3T_1)$ and $^3B_1(^3A_2) \rightarrow {}^3E(^3T_2)$ transitions are sensitive to dopant concentrations. We suggest that the fluence of locally uncompensated Me^{2+} ions and oxygen vacancies are responsible for these variations.

Absorption from metastable excited state $^3B_2(^3T_2)$ in the Cr^{4+} center is negligible. Linear losses due to absorption of other centers in crystals with high chromium concentration and the calcium dopant are found.

[1] E. P. Alleev, N. B. Angert, N. I. Borodin, V. M. Garmash, V. A. Zhitnyuk, V. N. Lukhina, O. G. Siyuchenko, and A. V. Shestakov, RF Patent No. 249398 (1987).

[2] N. B. Angert, N. I. Borodin, V. M. Garmash, V. A. Zhitnyuk, A. G. Okhrimchuk, O. G. Siyuchenko, and A. V. Shestakov, Kvant. Elektron. (Moscow) **15**, 113 (1988) [Sov. J. Quantum Electron. **18**, 73 (1988)].

[3] K. Spariosu, W. Chen, R. Stultz, and M. Birnbaum, Opt. Lett. **18**, 814 (1993).

[4] N. I. Borodin, V. A. Zhitnyuk, A. G. Okhrimchuk, and A. V. Shestakov, Izv. Akad. Nauk SSSR, Ser. Fiz. **54**, 1500 (1990) [Bull. Acad. Sci. USSR, Phys. Ser. **54**, 54 (1990)].

[5] P. M. W. French, N. H. Risvi, J. R. Taylor, and A. V. Shestakov, Opt. Lett. **18**, 39 (1993).

[6] N. I. Borodin, A. G. Okhrimchuk, and A. V. Shestakov, in *OSA Proceedings on Advanced Solid State Lasers*, edited by L. L. Chase and A. A. Pinto (OSA, Washington, DC, 1992), Vol. 13, pp. 42–46.

[7] M. I. Demchuk, N. V. Kuleshov, V. P. Mihailov, A. I. Mit'kovets, P. V. Prokoshyn, V. A. Sandulenko, A. P. Shkadarevich, and K. V. Yumashev, Zh. Prikl. Specktrosk. **51**, 337 (1989).

[8] H. Eilers, U. Hommerich, S. M. Jacobsen, and W. M. Yen, in *OSA Proceedings on Advanced Solid State Lasers*, edited by A. A. Pinto and T. Y. Fan (OSA, Washington, DC, 1993), Vol. 15, pp. 437–440.

[9] V. M. Garmash, V. A. Zhitnyuk, A. G. Okhrimchuk, and A. V. Shestakov, Izvest. Acad. Nauk. SSSR **26**, 1700 (1990) [Inorg. Mater. **26**, 1448 (1990)].

[10] K. R. Hoffman, U. Hommerich, S. M. Jacobsen, and W. M. Yen, J. Lumin. **52**, 227 (1992).

[11] S. Kuck, V. Pohlmann, K. Petermann, G. Huber, and T. Schonherr, J. Lumin **60&61**, 192 (1994).

[12] S. Kuck, K. Petermann, and G. Huber, in *OSA Proceedings on Advanced Solid State Lasers*, edited by G. Dube and L. L. Chase (OSA, Washington, DC, 1991), Vol. 10, pp. 92–94.

[13] A. G. Okhrimchuk and A. V. Shestakov, Opt. Mater. **3**, 1 (1994).

[14] A. G. Okhrimchuk, A. V. Shestakov, and V. A. Zhitnyuk, Electronic Technique, Laser Technique and Optoelectronics series (in Russian) **54**, 20 (1990).

[15] A. Sugimoto, Y. Nobe, and K. Yamagishi, J. Cryst. Growth **140**, 349 (1994).

[16] B. M. Tissue, W. Jia, L. Lu, and W. M. Yen, J. Appl. Phys. **70**, 3775 (1991).

[17] L. I. Krutova, N. A. Kulagin, V. A. Sandulenko, and A. V. Sandulenko, Sov. J. Solid State Phys. **31**, 170 (1989).

[18] H. Eilers, U. Hommerich, S. M. Jacobsen, and W. M. Yen, Phys. Rev. B **49**, 15 505 (1994).

[19] H. Eilers, K. R. Hoffman, W. M. Dennis, S. M. Jacobsen, and W. M. Yen, Appl. Phys. Lett. **61**, 2958 (1992).

[20] A. G. Okhrimchuk, D. V. Smolin, and A. V. Shestakov (unpublished).

[21] V. M. Garmash, N. I. Borodin, L. A. Ermakova, V. A. Zhitnyuk, A. G. Okhrimchuk, S. V. Protasova, and A. V. Shestakov, Electronic Technique, Laser Technique and Optoelectronics series (in Russian) **51**, 20 (1989).

[22] S. Camacho-Lopez, R. P. M. Green, G. J. Crofts, and M. J. Damzen, J. Mod. Opt. **44**, 209 (1997).

[23] M. G. Brik and D. G. Shchekoldin, Opt. Spectrosk. (St. Petersburg) **84**, 760 (1998) [Opt. Spectrosc. **84**, 683 (1998)].